On Computing Smooth Solutions of DAE's for Elastic Multibody Systems

W. C. Rheinboldt[1] and B. Simeon[2,3]

Abstract: Multibody systems are considered which involve combinations of rigid and elastic bodies. Discretizations of the PDEs, describing the elastic members, lead to a semidiscrete system of ODEs or DAEs. Asymptotic methods are introduced which provide a theoretical basis of various known engineering results for the ODE case. These results are then extended to the DAE case by means of suitable local ODE representations. The recently developed MANPAK algorithms for computations on implicitly defined manifolds form the basic tools for a computational method which provides consistent approximate solutions of the semidiscrete DAE that satisfy all constraints and are close to the smooth motion and an average solution. Several numerical examples indicate the effectiveness of this asymptotic method for elastic multibody systems.

1 Introduction

Standard mechanical multibody systems involve collections of several bodies which are interconnected either by joints that constrain the relative motion of pairs of bodies, or by springs and dampers that act as compliant elements. Mathematical models for systems of rigid bodies have been developed and analysed at least since the eighteenth century. But, increasingly in recent years, combinations of rigid and elastic bodies are being considered as well. These so-called *elastic* or *flexible multibody systems* are aimed at the growing demands for refined simulations in vehicle dynamics, robotics, and air- and space-craft development (see, e.g., [3, 15]).

The mathematical models of such elastic multibody systems represent combined system of differential-algebraic equations (DAEs) and partial differential equations (PDEs). Here the PDEs are the standard equations of elasto-mechanics describing the deformations of the elastic bodies while the DAEs model the motion of the rigid bodies and the constraints defined by all the joimts of the system. Usually, in practice, the deformations of the elastic members are assumed to be small in comparison to the gross-motion; that is, to the spatial

[1]Dept. of Mathematics, Univ. of Pittsburgh, Pittsburgh, PA, USA

[2]FB Mathematik, TU-Darmstadt, Darmstadt, Germany

[3]The work of this author was supported in part by a grant of DAAD Bonn, Germany.

translations and rotations. Moreover, contact problems and friction are neglected; that is, all joints attached to elastic bodies are treated as rigid body interconnections.

Simulation methods for elastic multibody system typically begin with a discretization of the PDEs corresponding to the elastic bodies. This reduces the overall equations of motion to an (extended) system of DAEs. The resulting semi-discretized system involves two types of state variables, namely, those for the gross-motion, on the one hand, and those for the elastic-deformations, on the other. They may be expected to have widely differing time scales, and, hence, the numerical integration of the system typically represents a challenging problem.

In the engineering literature, several methods for the simulation of elastic multibody systems have been discussed. In most cases, it is assumed that the semi-discretized equations of motion form a global system of ODEs; that is, that suitable (minimal) coordinates have been chosen. Moreover, besides an assumption of small deformations, model reduction techniques are frequently utilized for efficiency reasons.

By considering the semi-discretized equations of elastic multibody systems as a singularly perturbed systems, we show here that asymptotic methods can be developed to provide a firm analysis of the standard engineering approaches in the ODE case, as, for instance, the so-called linear theory of elasto-dynamics in [16]. Then this asymptotic approach is extended to the general DAE case by using suitable local ODE representations. More specifically, by means of the MANPAK algorithms of [13], a computational method is developed which constructs suitable local coordinate systems and in turn allows for the application of the expansion steps of the earlier discussed ODE case. In this way, consistent approximations are obtained that satisfy all constraints and are close to the smooth motion and an average solution.

Section 2 presents the mathematical model and shows the connection to stiff mechanical systems. Then, in Section 3, the indicated asymptotic approach for models in ODE form is introduced. Section 4 extends these results to the general DAE case in a form that exhibits directly the overall computational approach. Finally, in Section 5 some numerical results are given for a slider crank and a truck model involving elastic parts.

2 Mathematical model

For the modelling of flexible multibody system we use here the standard formulations underlying several simulation programs, [7, 15, 20], and refer for some further details about these mathematical models also to [3, 18, 19]. As noted in the Introduction, for the computation the PDEs describing the elastic members of the system are discretized in space, for instance, by means of a finite element approximation. Since our interest here is in the time integration problem, we shall assume that this discretization is already in place and hence that the equations of motion are given in a semi-discretized form.

For any given time t, let $p(t) \in \mathbf{R}^{n_p}$ denote the vector of the position and orientation of all bodies and $q(t) \in \mathbf{R}^{n_q}$ that describing the deformation of the elastic bodies which have been discretized in space with respect to body-fixed reference frames. Then the equations of motion have the following form of a partitioned DAE

$$
\begin{aligned}
\begin{pmatrix} M_r(p,q) & C(p,q)^T \\ C(p,q) & M_\Delta \end{pmatrix} \begin{pmatrix} \ddot{p} \\ \ddot{q} \end{pmatrix} &= \begin{pmatrix} f_r(p,q,\dot{p},\dot{q},t) \\ f_\Delta(p,q,\dot{p},\dot{q},t) - \text{grad } W_\Delta(q) \end{pmatrix} - G(p,q)^T \lambda \\
0 &= g(p,q)
\end{aligned} \qquad (1)
$$

Here, $M_r(p,q) \in \mathbf{R}^{n_p \times n_p}$ and $M_\Delta \in \mathbf{R}^{n_q \times n_q}$ represent mass matrices, $C(p,q) \in \mathbf{R}^{n_q \times n_p}$ is a coupling matrix, $f_r(p,q,\dot{p},\dot{q},t) \in \mathbf{R}^{n_p}$ and $f_\Delta(p,q,\dot{p},\dot{q},t) \in \mathbf{R}^{n_q}$ characterize the applied and external forces, and $W_\Delta(q)$ defines the strain energy of the discretized elastic bodies. Finally, $g(p,q) \in \mathbf{R}^{n_\lambda}$ specifies the holonomic constraints, $G(p,q) := (D_p\, g(p,q), D_q\, g(p,q))$ is the $n_\lambda \times (n_p + n_q)$ Jacobian of these constraints, and $\lambda(t) \in \mathbf{R}^{n_\lambda}$ a corresponding vector of Lagrange multipliers. Throughout this presentation we shall assume that the mappings M_r, C, f_r, f_Δ, W_Δ and g are sufficiently smooth.

Note that the DAE (1) includes several important limiting cases. When the deformation q vanishes – and, for simplicity, the arguments $q \equiv 0$ and $\dot{q} \equiv 0$ are omitted – then (1) reduces to the classical Euler-Lagrange equations for systems of rigid bodies:

$$
\begin{aligned}
M_r(p)\,\ddot{p} &= f_r(p,\dot{p},t) - G(p)^T \lambda \\
0 &= g(p).
\end{aligned} \qquad (2)
$$

On the other hand, for a vanishing gross-motion p, we arrive (under suitable assumptions) at the equations of structural dynamics ([5])

$$
M_\Delta \ddot{q} = -\text{grad } W_\Delta(q) + f_\Delta(t). \qquad (3)
$$

These equations may be derived directly by a discretization of Cauchy's first law of motion

$$\rho\, u_{tt} = \text{div } P + \beta, \tag{4}$$

together with appropriate boundary conditions and material laws. Here $u(x,t)$ denotes the displacement field, ρ is the mass density, β the density of the body forces, and $P(x,t)$ the first Piola-Kirchhoff stress tensor.

In (1) (as well as (3)) it is usual to assume linear elasticity with strain energy $W_\Delta(q) = 1/2q^T K_\Delta q$ involving a symmetric positive definite stiffness matrix $K_\Delta \in \mathbf{R}^{n_q \times n_q}$. While many elastic multibody systems are within this framework, there are applications where additional nonlinear elasticity terms are required, as, for example, when the effects of geometric stiffening are to be modelled (see e.g. [20]). Accordingly, we consider here more general elastic potentials W_Δ that have a positive definite Hessian $D^2 W_\Delta(q)$ and for which grad $W_\Delta(q) = 0$ implies that $q = 0$.

Since the equations of motion (1) have the general structure of the Euler-Lagrange equations, it is easy to show that the DAE has index three provided the matrix

$$\begin{pmatrix} \begin{bmatrix} M_r(p,q) & C(p,q)^T \\ C(p,q) & M_\Delta \end{bmatrix} & G(p,q)^T \\ G(p,q) & 0 \end{pmatrix} \tag{5}$$

is invertible along any solution. In view of the many available algorithms for computing solutions of the Euler-Lagrange equations for rigid body systems, it may appear that also the numerical solution of the general DAE (1) is easily accomplished. However, this is typically not the case, since, due to its mixed structure, the solutions of (1) often exhibit strongly differing time scales; that is, the system turns out to be stiff.

Stiff mechanical system

The stiffness of the equations of motion (1) is frequently due to a stiff potential, when the strain energy may be written as $W_\Delta(q) = \varepsilon^{-2} U(z)$ where the size of the ε depends on model parameters, such as the modulus of elasticity, as well as on geometry data. With the notation $z = (p,q)$, the system (1) then has the form

$$\begin{aligned} M(z)\,\ddot{z} &= f(z,\dot{z},t) - \frac{1}{\varepsilon^2}\,\text{grad } U(z) - G(z)^T\lambda \\ 0 &= g(z)\,, \end{aligned} \qquad \varepsilon \ll 1\,. \tag{6}$$

Lubich [10] considered the ODE case of (6); that is, stiff mechanical systems without constraint equations, and studied, in particular, the use of Runge-Kutta methods. More recently, Bornemann [1] investigated the asymptotic behavior of this DAE for conservative systems; that is, when (6) is derived from a Lagrangian

$$\mathcal{L}(z, \dot{z}) = \frac{1}{2}\langle \dot{z}, \dot{z}\rangle - V(z) - \frac{1}{\varepsilon^2}\, U(z)$$

on the manifold $\mathcal{M} = \{z \in \mathbf{R}^n : 0 = g(z)\}$, $n = n_p + n_q$. The central question addressed there is the behavior of the dynamical system in the limit $\varepsilon \to 0$. If the submanifold

$$\mathcal{N} = \{z \in \mathbf{R}^n \;:\; g(z) = 0,\ \mathrm{grad}\ U(z) = 0\} \subset \mathcal{M}$$

is non-empty, the solutions will, in general, oscillate on a time scale of order $\mathcal{O}(\varepsilon)$ around $\mathcal{N}$. As shown in [1], there exists a limiting or 'homogenized' system with solutions in $\mathcal{N}$ for a large class of potentials U.

In the case of the equations of motion (1) with $W_\Delta(q) = \varepsilon^{-2}U(z)$, the set $\mathcal{N}$ turns out to be the rigid motion space since we assumed that grad $W_\Delta(q) = 0$ implies that $q = 0$. In addition, due to the structure of the strain energy W_Δ, no 'correcting potential' is generally needed, even in the case of nonlinear elasticity. In other words, when (1) is viewed as a stiff mechanical system, its limit is – as naturally expected – the rigid body system (2).

These observations suggest that we should not consider the case $\varepsilon \to 0$ but, instead, seek to approximate solutions for nonzero, but small ε. Clearly, in order to utilize the expected asymptotic behavior, the submanifold $\mathcal{N} \subset \mathcal{M}$ will have to be non-empty. A sufficient condition for this is that the matrix

$$\begin{pmatrix} 0 & D^2 W_\Delta(q) \\ D_p g(p,q) & D_q g(p,q) \end{pmatrix} \tag{7}$$

has full rank whence, in particular, $D_p\, g(p,q)$ must have full rank n_λ. In other words, we are postulating a transversality condition for the configuration space and the constraining stiff potential.

Other models and remarks

Irrespective of the specification of the stiff potential, the DAE (1) may, by itself, be considered as a limiting case of a singularly perturbed ODE. In fact, if the joints were not described by constraints but by certain elastic interconnections, then the resulting semi-discretized equations would form an ODE involving additional stiffness parameters for the joint elasticities. For instance, a simple form of the elastic connections leads to a problem

$$M(z)\, \ddot{z} = f(z, \dot{z}, t) - \frac{1}{\varepsilon^2}\ \mathrm{grad}\ U(z) - \frac{1}{\mu^2}\ \mathrm{grad}\left(\|g(z)\|_2^2\right) \tag{8}$$

where both ε and μ are small. Here, typically the effects of the joint elasticities are an order smaller than the elastic deformations; that is, we have $\mu \ll \varepsilon$. There appears to be little known about the asymptotics of such systems involving a vector of small parameters. This is probably due to the fact – already observed in simple examples – that the asymptotic behavior depends critically on the way the parameter vector tends to zero.

Another noteworthy point is that not all deformation modes of an elastic body necessarily induce a singular perturbation. For instance, let $\omega_1 \leq \omega_2 \leq \ldots \leq \omega_{n_q}$ be the eigenvalues of the elastic members in the linear case; that is, the solutions of the eigenvalue problem $\omega^2 M_\Delta q = K_\Delta q$. The eigenvectors define a transformation matrix T such that

$$T^T M_\Delta T = I, \qquad T^T K_\Delta T = \mathrm{diag}\,(\omega_1^2, \ldots, \omega_{n_q}^2)\,, \tag{9}$$

where I denotes the identity matrix. Frequently, there is an index k such that the frequencies $\omega_1, \ldots, \omega_k$ are in the time scale of the gross-motion p, and the higher frequencies $\omega_{k+1}, \ldots, \omega_{n_q}$ represent stiff modes. A standard example is here a beam with both bending (slow) and lengthening (fast) modes. Using the transformation (9) and rearranging the unknowns such that p contains exactly the slow deformation modes and q only the fast or stiff ones, we can view the equations of motion again as a perturbed system. In the ODE case, this has been an approach used in [14]. In such a partioned system where q contains only the fast modes, the process of going to the limit $\varepsilon \to 0$ corresponds to the frequently used alternative of reducing the dimension and complexity of the model by chopping off simply all higher frequencies [8].

Finally, we observe that multibody systems are in general not conservative. Dissipation may appear not only in such interconnection elements as dampers but also in elastic body models. Concerning the latter, we shall always assume that the damping terms are small in comparison to the force term $-\mathrm{grad}\; W_\Delta(q)$.

3 The ODE case

Assume that the equations of motion (1) are given as an unconstrained system

$$\begin{pmatrix} M_r(p,q) & C(p,q)^T \\ C(p,q) & M_\Delta \end{pmatrix} \begin{pmatrix} \ddot p \\ \ddot q \end{pmatrix} = \begin{pmatrix} f_r(p,q,\dot p,\dot q,t) \\ f_\Delta(p,q,\dot p,\dot q,t) \end{pmatrix} - \frac{1}{\varepsilon^2} \begin{pmatrix} 0 \\ \mathrm{grad}\; W(q) \end{pmatrix} \tag{10}$$

with a symmetric positive definite mass matrix on the left and a stiff elastic potential $\varepsilon^{-2} W(q) = W_\Delta(q)$, $\varepsilon \ll 1$. This partitioned ODE (10) belongs to a class of singularly perturbed systems

$$M(z)\,\ddot{z} = f(z,\dot{z},t) - \frac{1}{\varepsilon^2}\,\text{grad}\;U(z) \tag{11}$$

considered in [10]. There the following assumptions were used:

(i) The mass matrix $M(z)$ is symmetric positive definite for all $z \in \mathbf{R}^n$.
(ii) There exists a non-empty, open set $E \subset \mathbf{R}^n$ such that $\mathcal{U} = \{z \in E : \text{grad}\;U(z) = 0\}$ is a d-dimensional sub-manifold of $\mathbf{R}^n$; thus U attains a (local) minimum at each $z \in \mathcal{U}$;
(iii) The potential U is strongly convex with respect to the $M(z)$-orthogonal complement of the tangent space $T_z\mathcal{U} = \ker D^2U(z)$; that is there exists $\alpha > 0$ such that

$$v^T D^2U(z)v \geq \alpha v^T M(z)v, \quad \forall v \in \{w \in \mathbf{R}^n \;:\; w^T M(z)u = 0, \forall u \in T_z\mathcal{U}\}.$$

Under these three conditions, the smooth motion z^ε is a sufficiently differentiable solution of (11) which, together with its derivatives, is bounded independently of ε and can be represented in the form of an outer expansion

$$z^\varepsilon(t) = z^0(t) + \varepsilon^2 z^1(t) + \varepsilon^4 z^2(t) + \ldots + \varepsilon^{2N} z^N(t) + O(\varepsilon^{2N+2}). \tag{12}$$

Here, the coefficient functions z^i are independent of ε and are generally specified as the solutions of a chain of DAE's, each of index three.

For the system of equations (10) we assumed already that (i) holds. It is easily verified that (ii) and (iii) are satisfied if the Hessian $D^2W(q)$ is positive definite. Note that the stiff force term $\varepsilon^{-2}\text{grad}\;W(q) = \text{grad}\;W_\Delta(q)$ vanishes on $\mathcal{U} = \{(p,q) \in \mathbf{R}^{n_p} \times \mathbf{R}^{n_q} : q = 0\}$. Now, when the expansion (12) is applied to (10) in the form

$$p^\varepsilon(t) = p^0(t) + \varepsilon^2 p^1(t) + \varepsilon^4 p^2(t) + \ldots\,, \qquad q^\varepsilon(t) = q^0(t) + \varepsilon^2 q^1(t) + \varepsilon^4 q^2(t) + \ldots\,, \tag{13}$$

then we obtain a chain of equations that define the coefficient functions for this particular case.

By Taylor expansion, the coefficient of ε^{-2} in (10) vanishes if

$$0 = \text{grad}\;W(q^0) \quad \Rightarrow \quad q^0 \equiv 0\,,$$

and the coefficient ε^0 provides the equation

$$M_r(p^0,0)\,\ddot{p}^{\,0} = f_r(p^0,0,\dot{p}^0,0,t)\,. \tag{14}$$

In other words, if p is identified with the gross motion and q with the elastic motion, then, as expected, the first coefficient functions p^0, q^0 define the rigid body motion with zero deformation (see (2)). In addition, when comparing coefficients of ε^0 in the second line of (10), we obtain a linear system for q^1,

$$D^2W(0)\,q^1 = f_\Delta(p^0, 0, \dot{p}^0, 0, t) - C(p^0, 0)\,\ddot{p}^{\,0}\,. \tag{15}$$

The next steps follow recursively and are omitted here since they involve higher derivatives that are typically not available in simulation programs.

The expansion steps derived thus far form the basis of a standard approach in the engineering literature, the so-called *decoupled quasi-static analysis,* [7]. Let

$$p^a(t) := p^0(t) \qquad\qquad q^a(t) := q^0(t) + \varepsilon^2 q^1(t) = \varepsilon^2 q^1(t) \tag{16}$$

denote the approximations given by the ODE of rigid motion (14) and the linear system (15), respectively. The second order system (14) can be solved for p^a by a standard ODE method and then, in a post-processing step, the corresponding elastic response q^a can be computed from the linear system

$$D^2W_\Delta(0)\,q^a = f_\Delta(p^a, 0, \dot{p}^a, 0, t) - C(p^a, 0)\,\ddot{p}^{\,a} \tag{17}$$

involving the stiffness matrix $D^2W_\Delta(0)$. Obviously, while this approach is efficient, it leaves the question of how well p^a and q^a approximate a solution. Both p^a and q^a are smooth and, by construction, we know that $p^a(t) - p^\varepsilon(t) = \mathcal{O}(\varepsilon^2)$, $q^a(t) - q^\varepsilon(t) = \mathcal{O}(\varepsilon^4)$. More interesting is a comparison of (p^a, q^a) with a possibly oscillatory solution (p, q) of (10). The following result, derived essentially from Theorem 2.2 of [10], provides an estimate.

Theorem 1. *Let (p^a, q^a) be the approximation (16) and (p, q) a solution of (10) for which the initial values satisfy $p(0) - p^a(0) = \mathcal{O}(\varepsilon^3)$, $\dot{p}(0) - \dot{p}^a(0) = \mathcal{O}(\varepsilon^2)$, $q(0) - q^a(0) = \mathcal{O}(\varepsilon^3)$, and $\dot{q}(0) - \dot{q}^a(0) = \mathcal{O}(\varepsilon^2)$. Then on bounded time intervals it follows that*

$$\begin{array}{rclcrcl} p(t) - p^a(t) &=& \mathcal{O}(\varepsilon^2), && \dot{p}(t) - \dot{p}^a(t) &=& \mathcal{O}(\varepsilon^2), \\ q(t) - q^a(t) &=& \mathcal{O}(\varepsilon^2), && \dot{q}(t) - \dot{q}^a(t) &=& \mathcal{O}(\varepsilon^2)\,. \end{array}$$

Proof: We use the main ideas of [10] but specialize, where necessary, to the system (10). First, a coordinate change is applied to simplify the structure of the potential W. Locally we have

$$W(q) - W(0) = \frac{1}{2} q^T D^2 W(0) q^T + r(q), \qquad r(q) = \mathcal{O}(\|q\|^3).$$

Let $LL^T = D^2W(0)$ be the Cholesky decomposition of the Hessian, then, with the new coordinates

$$w := \omega(q) L^T q, \qquad \omega(q) := \left(1 + \frac{r(q)}{q^T D^2 W(0) q}\right)^{1/2},$$

it follows that

$$W(q) = \frac{1}{2} w^T w + \text{const}.$$

Without loss of generality we assume from now on that grad $W(q) = q$ but otherwise retain the notation. The approximation (p^a, q^a) inserted into (10) has a defect of order $\mathcal{O}(\varepsilon^2)$, and hence the differences $\Delta p := p - p^a$ and $\Delta q := q - q^a$ satisfy

$$M(t) \begin{pmatrix} \ddot{\Delta p} \\ \ddot{\Delta q} \end{pmatrix} = \mathcal{O}(\Delta p) + \mathcal{O}(\Delta q) + \mathcal{O}(\dot{\Delta p}) + \mathcal{O}(\dot{\Delta q}) - \frac{1}{\varepsilon^2} \begin{pmatrix} 0 \\ \Delta q \end{pmatrix} + \mathcal{O}(\varepsilon^2) \tag{18}$$

where

$$M(t) = \begin{pmatrix} M_r(p^a, q^a) & C(p^a, q^a)^T \\ C(p^a, q^a) & M_\Delta \end{pmatrix}.$$

Let $Q(t)$ be an orthogonal matrix such that

$$Q(t)^T M(t)^{-1/2} \begin{pmatrix} 0 & 0 \\ 0 & I_{n_q} \end{pmatrix} M(t)^{-1/2} Q(t) = \begin{pmatrix} 0 & 0 \\ 0 & B(t) \end{pmatrix},$$

then, clearly, the $n_q \times n_q$ matrix $B(t)$ is positive definite and both B and Q are smooth functions of t. With

$$\begin{pmatrix} \delta \\ \eta \end{pmatrix} := Q(t)^T M(t)^{1/2} \begin{pmatrix} \Delta p \\ \Delta q \end{pmatrix}$$

it follows from (18)

$$\ddot{\delta} = \mathcal{O}(\|\delta\| + \|\dot{\delta}\| + \|\eta\| + \|\dot{\eta}\|) + \mathcal{O}(\varepsilon^2) \tag{19}$$

$$\ddot{\eta} = -\varepsilon^{-2} B(t)\eta + \mathcal{O}(\|\delta\| + \|\dot{\delta}\| + \|\eta\| + \|\dot{\eta}\|) + \mathcal{O}(\varepsilon^2). \tag{20}$$

Let $B(t) = R(t)R(t)^T$ be a smooth Cholesky decomposition of $B(t)$. Then in terms of the new variable

$$\xi := \begin{pmatrix} \eta \\ \varepsilon R(t)^{-1} \dot{\eta} \end{pmatrix}$$

we are finally led to the first order system

$$\dot{\xi} = \frac{1}{\varepsilon} \begin{pmatrix} 0 & R(t) \\ -R(t)^T & 0 \end{pmatrix} \xi + \mathcal{O}(\|\xi\| + \varepsilon(\|\delta\| + \|\dot{\delta}\|)) + \mathcal{O}(\varepsilon^3).$$

The skew-symmetry of the matrix on the right allows here for an energy estimate (Gronwall inequality). More specifically, for initial values $\xi(0) = \mathcal{O}(\varepsilon^3)$, we obtain

$$\|\xi(t)\| \le C\varepsilon \int_0^t (\|\delta(\tau)\| + \|\dot{\delta}(\tau)\|) d\tau + \mathcal{O}(\varepsilon^3)$$

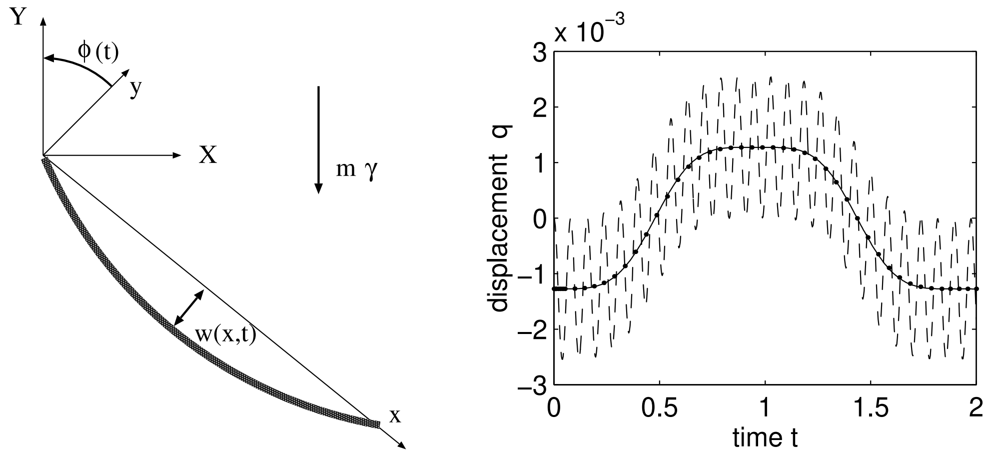

Figure 1. Elastic pendulum. Left: Inertial and body-fixed coordinate systems. Right: Oscillatory (dashed) and smooth (solid) solutions for $\varepsilon = 0.02$, $\gamma = 10$.

and

$$\|\eta(t)\| + \|\dot{\eta}(t)\| \leq C \int_0^t (\|\delta(\tau)\| + \|\dot{\delta}(\tau)\|)d\tau + \mathcal{O}(\varepsilon^2).$$

With the latter bound inserted into (19) and with $\dot{\delta} = \sigma$ and the Dini derivative D_+ this leads to

$$\begin{aligned} &D_+\|\delta(t)\| \leq \|\sigma(t)\|, \\ &D_+\|\sigma(t)\| \leq C_1(\|\delta(t)\| + \|\sigma(t)\|) + C_2 \textstyle\int_0^t (\|\delta(\tau)\| + \|\sigma(\tau)\|)d\tau + \mathcal{O}(\varepsilon^2)\,. \end{aligned}$$

When the inequality is replaced by an equality, then the resulting integro-differential system satisfies the standard monotonicity requirements of [21], p. 122. Thus from the results of [21] we conclude that, on bounded time intervals, it follows that

$$\delta(t) = \mathcal{O}(\varepsilon^2), \qquad \sigma(t) = \mathcal{O}(\varepsilon^2),$$

for any initial values such that $\delta(0) = \mathcal{O}(\varepsilon^2)$, $\sigma(0) = \mathcal{O}(\varepsilon^2)$. □

In Theorem 1 the initial values play a crucial role. If $p(0)$ and $q(0)$ are further away from the approximate smooth motion, then the resulting estimate will become much worse. In particular, if we start with $q(0) = 0$ on a rigid motion trajectory, then we encounter strong oscillations in the fast time scale. Of course, as the deformation variables are themselves generally of order $\mathcal{O}(\varepsilon^2)$, the above estimate for q is worse than the one for p. In essence, this means that q may oscillate around q^a with an amplitude of order $\mathcal{O}(\varepsilon^2)$.

Example The planar elastic pendulum of Fig. 1 consists of a long rod that vibrates in its plane. The left end is attached to a rotational joint placed at the origin of the inertial reference frame. If the length l is much larger than either of the cross sectional dimensions h (height) and b (width), the lateral displacement $w(x,t)$ with respect to the body-fixed reference frame is characterized by the dispersive wave equation [2]

$$\rho\, A\, w_{tt} \;+\; E\, I\, w_{xxxx} \;=\; 0$$

where ρ denotes the mass density, $A = bh$ is the cross section area, E the elasticity modulus, and $I = (1/12)bh^3$ the axial moment of inertia. For pin-pin boundary conditions $\psi(0) = \psi(l) = 0$, the usual ansatz $w(x,t) = \psi(x)\, q(t)$ leads to the eigenfunctions $\psi(x) = \sin(k\pi x/l)$ corresponding to the eigen-frequencies $\omega_k = k^2(\pi/\ell)^2\sqrt{EI/(\rho A)}$, $k = 1, 2, \ldots$. We consider only the first mode $w(x,t) = \sin(\pi x/l)q(t)$ for the frequency $\omega = \omega_1$ and set, for simplicity, $\ell = 1$, $\rho bh = 1$. Then, in terms of the deformation variable q and the gross motion coordinate ϕ, and with $\varepsilon := 1/\omega$ the equations of motion are

$$\begin{aligned} (\frac{2}{3} + q^2)\ddot{\phi} + \bar{\pi}\ddot{q} &= -\gamma\cos\phi + 2\bar{\pi}\gamma\sin\phi\, q - 2q\dot{\phi}\dot{q} \\ \bar{\pi}\ddot{\phi} + \ddot{q} &= -2\bar{\pi}\gamma\cos\phi + q\dot{\phi}^2 - \frac{1}{\varepsilon^2}q\,, \quad \bar{\pi} = \frac{2}{\pi},\ \gamma \text{ gravity const.} \end{aligned} \tag{21}$$

Evidently, (21) includes the linear oscillator and the rigid pendulum equations as special cases. The latter coincides with the equation for ϕ^a defined in (14) while q^a follows from (17); that is,

$$2/3\ddot{\phi}^{\,a} = -\gamma\cos\phi^a, \qquad q^a = \varepsilon^2\left(-2\bar{\pi}\gamma\cos\phi^a - \bar{\pi}\ddot{\phi}^{\,a}\right).$$

The right part of Fig. 1 shows the solutions q of (21) for initial values $\phi(0) = \phi^a(0) = 0$, $q(0) = q^a(0)$ (solid line) and $\phi(0) = 0$, $q(0) = 0$ (dashed line), respectively. In both cases, the initial velocities were chosen to be zero. While the solution for $q(0) = q^a(0)$ cannot be distinguished from the smooth approximation q^a (dotted line), the initial condition $q(0) = 0$ results in fast oscillations around q^a. Note that an inner expansion in the time scale t/ε provides for small $\dot{\phi}$

$$q(t) = q^a(t) + (q(0) - q^a(0))\cos(\alpha/\varepsilon\cdot t) + \mathcal{O}(\varepsilon^3), \qquad \alpha = \sqrt{\pi^2/(\pi^2-6)}. \tag{22}$$

Thus, in agreement with Theorem 1, the difference $q(0) - q^a(0)$ determines the solution behavior. □

The elastic pendulum example illustrates that the approximation (p^a, q^a) may already be close to the true solution. If not, then it is at least possible to provide in this way initial values close to the smooth motion trajectory. The example shows also that a variant of the decoupled analysis, the so-called *linear theory of elastodynamics* [16], may result in erroneous results. The latter approach also begins with the rigid motion p^a and then solves the dynamic equation

$$M_\Delta \ddot{q}^{\,b} = f_\Delta(p^a, 0, \dot{p}^a, 0, t) - D^2 W_\Delta(0)\, q^b - C(p^a, 0)\, \ddot{p}^{\,a} \tag{23}$$

for q^b by means of finite element software. Due to the coupling matrix C, the frequencies in (10) and (23) are, in general, not the same. In the pendulum example, (10) is characterized by a shifted frequency $\alpha\omega$ (see (22)), while the system (23) has the frequency ω.

4 The DAE case

We return now to the constrained equations of motion (1) and – as in the previous section – consider the stiff case where the elastic potential is written as $W_\Delta(q) = \varepsilon^{-2} W(q)$, with $\varepsilon \ll 1$. Once again, an approximation of the smooth motion is sought which can be employed both for computing initial values and for post-processing the rigid motion. The discussion of Section 2 already indicated that singularly perturbed DAEs, such as (6), are far more complicated than ODEs. In fact, the literature in this area is rather sparse, and we are only aware of [1] and [22] where some first results have been derived. However, in our setting, it turns out that, under the full-rank condition for the matrix (7), we can derive a local ODE representation that preserves the partitioned structure. As noted in the Introduction, we will utilize the MANPAK algorithms of [13] to develop a computational method for constructing suitable local coordinate systems and then apply the expansion steps of Section 3 to the resulting local ODEs.

The existence of a structure-preserving local parametrization can be shown in a way exhibiting directly a computational approach. Let $E_p \subset \mathbf{R}^{n_p}$, $E_q \subset \mathbf{R}^{n_q}$ be nonempty, open sets such that E_q contains the origin and $\mathcal{M} = \{(p,q) \in E_p \times E_q : 0 = g(p,q)\}$ includes the rigid motion space of interest. As before, we require that the matrix (5) is invertible for any $(p,q) \in \mathcal{M}$ whence $\mathcal{M}$ is a submanifold of $\mathbf{R}^{n_p} \times \mathbf{R}^{n_q}$ of dimension $n_p + n_q - n_\lambda$. In addition, as indicated above, the matrix (7) is assumed to have full rank for $(p,q) \in \mathcal{M}$ which implies, in particular, that $\mathrm{rank} D_p g(p,0) = n_\lambda$.

Let $(p_0, 0) \in \mathcal{M}$ and $((p_0,0),(v_0,0)) \in T\mathcal{M}$ be some given rigid motion points on the manifold $\mathcal{M}$ and its tangent bundle $T\mathcal{M}$, respectively. Since $D_p g(p_0,0)$ has rank n_λ, the implicit function theorem guarantees that there exists a local parametrization $(\mathcal{V}, \varphi)$ of $\mathcal{M}$ near $(p_0, 0)$,

$$\varphi : \mathcal{V} \subset \mathbf{R}^{n_p - n_\lambda} \times E_q \to \varphi(\mathcal{V}) \subset \mathcal{M}, \quad \varphi(y,q) = (p,q), \tag{24}$$

where $\mathcal{V}$ is an open neighborhood of the origin. Then $(\mathcal{V} \times \mathbf{R}^{n_p-n_\lambda} \times \mathbf{R}^{n_q}, (\varphi, D\varphi))$ is a local parametrization of the tangent bundle near $((p_0, 0), (v_0, 0))$. For details we refer to [13].

For $(y, q) \in \mathcal{V}$ and velocities $(u, w) \in \mathbf{R}^{n_p-n_\lambda} \times \mathbf{R}^{n_q}$, consider now the mappings defined by

$$M(y,q) = \begin{pmatrix} M_r(\varphi(y,q)) & C(\varphi(y,q))^T \\ C(\varphi(y,q)) & M_\Delta \end{pmatrix},$$

$$b(y,q,u,w) = \begin{pmatrix} f_r(\varphi(y,q), D\varphi(y,q)(u,w)^T, t) \\ f_\Delta(\varphi(y,q), D\varphi(y,q)(u,w)^T, t) \end{pmatrix} - M(y,q)D^2\varphi(y,q)\big((u,w)^T, (u,w)^T\big).$$

Then, as shown in [13], the DAE (1) is locally equivalent to

$$\begin{aligned} \dot{y} &= u \\ \dot{q} &= w \\ \big(M(y,q)D\varphi(y,q), \quad G(\varphi(y,q))^T\big) \begin{pmatrix} \dot{u} \\ \dot{w} \\ \lambda \end{pmatrix} &= b(y,q,u,w) - \begin{pmatrix} 0 \\ \text{grad } W_\Delta(q) \end{pmatrix}. \end{aligned} \tag{25}$$

This first order system will be the basis for the algorithm outlined below. Since, by construction, $G(\varphi(y,q))D\varphi(y,q) = 0$ for $(y,q) \in \mathcal{V}$, the invertibility of the matrix (5) implies that of the matrix on the left of (25). Furthermore, $D\varphi$ has the form

$$D\varphi(y,q) = \begin{pmatrix} A(y,q) & B(y,q) \\ 0 & I_{n_q} \end{pmatrix}, \quad A(y,q) \in \mathbf{R}^{n_p \times (n_p - n_\lambda)}, \;\; B(y,q) \in \mathbf{R}^{n_p \times n_q}.$$

Thus, by premultiplying (25) from the left by $D\varphi^T$, we obtain – omitting for simplicity the arguments – the system

$$\begin{pmatrix} A^T M_r A & A^T(M_r B + C^T) \\ (B^T M + C)A & B^T C^T + CB + M_\Delta \end{pmatrix} \begin{pmatrix} \ddot{y} \\ \ddot{q} \end{pmatrix} = b - \begin{pmatrix} 0 \\ \text{grad } W_\Delta \end{pmatrix} \tag{26}$$

which has the partitioned structure of the ODE (10) with a symmetric positive definite mass matrix. In summary, this proves the following result:

Theorem 2. *Suppose that for $(p,q) \in \mathcal{M}$ the matrix (5) is invertible and (7) has full rank. Then, near any $(p_0, 0) \in \mathcal{M}$ and $((p_0,0),(v_0,0)) \in T\mathcal{M}$, there exists a local parametrization such that the DAE (1) can be written as the partitioned ODE (10).*

It should be noted that there is a slight difference between the local ODE (26) and the partitioned system (10) of Section 3. In fact, in (26) the lower right block of the mass matrix depends on the states $(y,q) \in \mathcal{V}$ while in (10) the corresponding block M_Δ is a constant matrix. This difference, however, plays no role in the method outlined below.

We now generalize the decoupled-analysis approach of Section 3 to the DAE case using the mentioned MANPAK algorithms of [13], notably the routines COBAS, GPHI, DGPHI and D2GPHI. Given a consistent discrete point with position $(p,0)$ and velocity $(v,0)$ on the rigid motion trajectory; that is, $(p,0) \in \mathcal{M}$ and $((p,0),(v,0)) \in T\mathcal{M}$, the method proceeds in three principal steps:

$$\begin{pmatrix} (p,0) \\ (v,0) \end{pmatrix} \xrightarrow{(\varphi,D\varphi)^{-1}} \begin{pmatrix} (0,0) \\ (u,0) \end{pmatrix} \xrightarrow{(17)} \begin{pmatrix} (0,q^a) \\ (u,w^a) \end{pmatrix} \xrightarrow{(\varphi,D\varphi)} \begin{pmatrix} (p^a,q^a) \\ (v^a,w^a) \end{pmatrix} \tag{27}$$

First, the local parametrization φ is constructed by the following algorithm:

Input $(p,0),(v,0)$;

1. Evaluate $G(p,0) = (D_p g(p,0), D_q g(p,0))$;
2. Use COBAS to compute the $n_p \times (n_p - n_\lambda)$ basis matrix U_p of $D_p g(p,0)$;
3. Add n_q canonical basis vectors to form the full basis matrix
   $U = \begin{pmatrix} U_p & 0 \\ 0 & I_{n_q} \end{pmatrix}$ of φ at $(p,0)$;
4. Set the local point $(y,q) = (0,0)$, $(u,w) = (U_p^T v, 0)$;

While the columns of U_p span the nullspace of $D_p g$ and define thus a tangent space parametrization, the same is, generally, not true of the full basis U. As long as (7) holds, however, the parametrization φ constructed in this way is well defined. For simplicity, autonomous constraints are assumed here but the implementation covers also time dependent constraints.

The second step evaluates the local representation (25) and computes the smooth motion approximation (17):

1. Use DGPHI to evaluate the derivative $D\varphi(0,0)$;
2. Use D2GPHI to evaluate the second derivative $D^2\varphi(0,0)\big((u,0)^T,(u,0)^T\big)$;
3. Evaluate $M(0,0)D\varphi(0,0) = \begin{pmatrix} M_r A & * \\ CA & * \end{pmatrix}$ and $b(0,0,u,0) = (b_r, b_\Delta)^T$;
4. Solve rigid local subsystem $\big(M_r A,\ (D_p\, g)^T\big)(\dot u, \lambda)^T = b_r$ for $\dot u$ and λ;
5. Solve $D^2 W_\Delta(0)\, q^a = b_\Delta - CA\dot u - (D_q\, g)^T \lambda$ for q^a;

The constraint derivative term $D^2g(p,0)\left((p,0)^T,(p,0)^T\right)$ is required to evaluate $D^2\varphi$. Moreover, $D^2\varphi$ is part of the right side b. Since (25) and (26) are equivalent, it is not necessary to calculate all the expressions and matrix products of (26). Instead, we exploit the block structure of $MD\varphi$ in (25) to compute first the rigid motion data $\dot{u}$ and λ and then the approximation q^a. Thus, altogether, two linear systems have to be solved, one of size n_p and one of size n_q.

The velocity $\dot{q}^a = w^a$ also plays an important role and cannot simply be set to zero. Differentiation of (17) provides an explicit expression for w^a but involves also higher derivative terms. Experience has shown that here an alternative approximation in terms of finite differences works well in practice. For this purpose, an additional rigid motion point with corresponding solution $\tilde{q}^a$ is computed either by a small integration step in the current local coordinate system or from data of a previous rigid motion simulation. Alternately, a finite difference approximation can also be based on several such points.

Finally, we apply the parametrization to obtain the approximation in global variables:

1. Use GPHI to compute the global point $\varphi(0,q^a) = (p^a,q^a)$;
2. Use DGPHI to evaluate $D\varphi(0,q^a)$;
3. Compute the global velocities $D\varphi(0,q^a)(u,w^a)^T = (v^a,w^a)^T$;

The algorithm GPHI uses a chord Newton method where the constraint Jacobian Dg and the basis matrix U form the iteration matrix of size n_p+n_q. Note that, in general, we will have $p^a \neq p$ and $v^a \neq v$.

The above, overall algorithm has been implemented in an experimental code. Besides the rigid motion point $(p,0)$ with velocity $(v,0)$, the user has to provide subroutines for evaluating M, g, G, D^2g, f_r, f_Δ, and the Hessian $D^2W_\Delta(0)$. The partition of the states into slow modes p and fast modes q is specified by a pointer variable and, hence, a change of this partition requires simply a shift of this pointer.

5 Computational examples

In this section we illustrate with two numerical examples the effectiveness of the asymptotic method developed in the previous section. The first example concerns a small slider crank model with only a few degrees of freedom while the second one involves a much larger model of a truck.

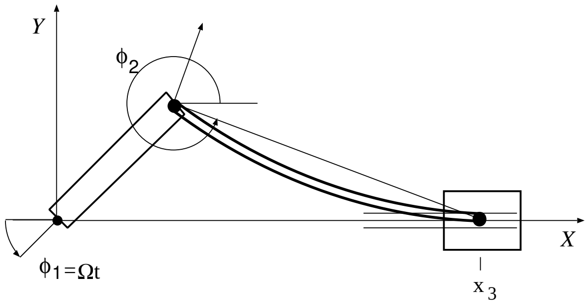

Figure 2: Slider crank mechanism.

Slider Crank

The planar slider crank mechanism of Fig. 2 consists of a rigid crank, an elastic connecting rod, a rigid sliding-block as well as two revolute and one translational joint [7]. The equations of motion form a partitioned differential-algebraic system (1) involving (i) $n_p = 3$ gross-motion coordinates

$$p := \begin{pmatrix} \phi_1 \\ \phi_2 \\ x_3 \end{pmatrix} \quad \begin{array}{l} \text{crank angle} \\ \text{connecting rod angle} \\ \text{sliding block displacement,} \end{array}$$

(ii) $n_q = 4$ deformation-coordinates

$$q := \begin{pmatrix} q_1 \\ q_2 \\ q_3 \\ q_4 \end{pmatrix} \quad \begin{array}{l} \text{first lateral mode} \sin(\pi x/l_2) \\ \text{second lateral mode} \sin(2\pi x/l_2) \\ \text{longitudinal displacement midpoint} \\ \text{longitudinal displacement endpoint,} \end{array}$$

and (iii) $n_\lambda = 3$ holonomic constraints for the inter-connection of crank and sliding block, and the prescribed crank motion $\phi_1 = \Omega(t)$. A detailed description of the model is found in [19], and, for test purposes, a FORTRAN subroutine is available at the IVPTestset [6]. The slider crank example has no dissipation and the eigen-frequencies of the elastic body are approximately

$$\omega_1 = 1277, \quad \omega_2 = 5107, \quad \omega_3 = 6841, \quad \omega_4 = 24613 \;\; [rad/s]\,.$$

In particular, the longitudinal displacements q_3 and q_4 are affected by the relatively large frequency ω_4.

For the case of a constant crank velocity $\dot{\phi}_1 = 150[rad/s]$, Figure 3 shows the behavior of solutions specified by different initial values. All solutions were computed by a numerical

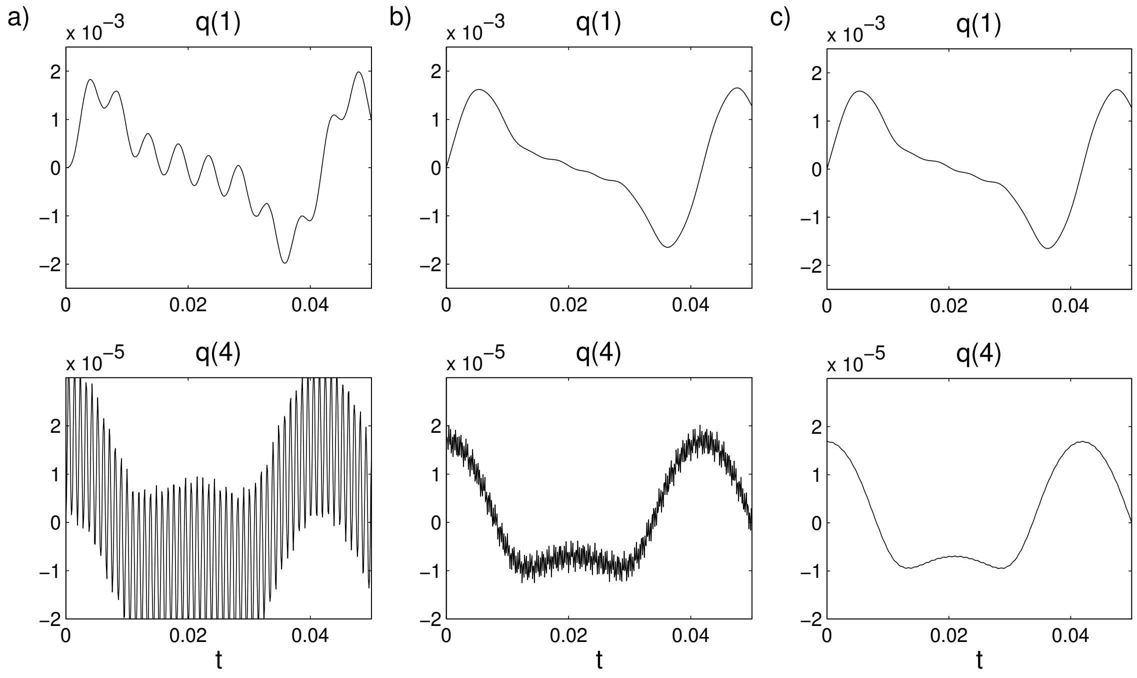

Figure 3: Solution behavior for different initial values, $\Omega(t) = 150 \cdot t$ (displacements in $[m]$).

integration of the full model (1) with the DAE integrator DAEQ3 of MANPAK. Since the stiffness is not very large, explicit discretization schemes remain applicable for the model. The gross-motion coordinates are not very sensitive and differ only slightly from those of a purely rigid-body model. However, the elastic body motion is strongly influenced by the choice of the initial values. In Fig. 3 a), the initial deformation was set to zero resulting in both lateral and longitudinal vibrations. In b), the initial values were computed by means of the index-one formulation of the DAE together with an expansion step (see Section 4) and a subsequent projection onto the constraint manifold. It turns out that the standard projection based on the 'natural metric', used in [9] and induced by the matrix (5), is not compatible with the stiff potential and, accordingly, the longitudinal modes still show some oscillatory behavior. Finally, in c) on the right, the algorithm of Section 4 was used to supply the initial values, and the resulting full solution is essentially smooth in all elastic coordinates. The algorithm was also applied for the computation of the smooth motion on the entire integration interval and the results are in very close agreement with those shown in c).

The quality of the approximation of the smooth motion over the entire interval depends mainly on the stiffness; that is, on the size of the perturbation parameter ε. From among various experiments we present in Figure 4 a simulation with a variable crank velocity. As

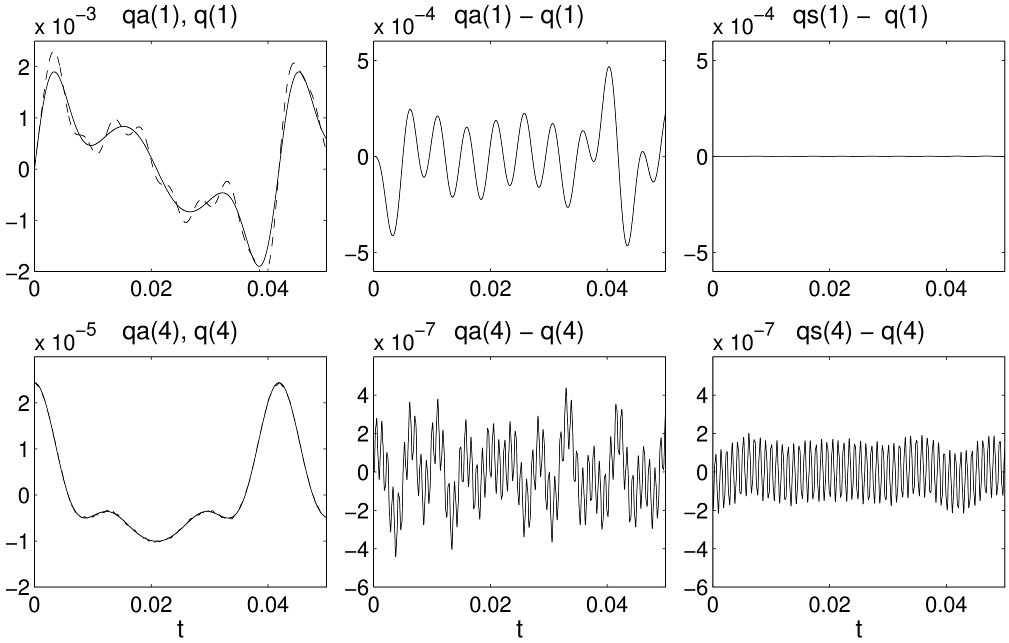

Figure 4: Full solution q and smooth approximation q^a for $\Omega(t) = 150t + 0.1 \cdot \sin(300t)$. On the right, q^s denotes the solution obtained with shifted partitioning.

in Fig. 3 c), the initial values were again supplied by the algorithm of Section 4. Since the corresponding ε is relatively large, the lateral displacement q_1, with its low frequency mode, is now slightly excited. In this case, the smooth motion approximation represents some average solution. At the same time, the very stiff longitudinal mode q_4 is well resolved. These results indicate that the partition of the variables used in the equations (1) is no longer adequate. We reran the test with a new grouping (p_s, q_s) of the variables where now p_s contains also the slow deformation modes q_1 and q_2 and only the stiff modes q_3 and q_4 are included in q_s. This is facilitated here by the block-diagonal structure of the stiffness matrix. The results, given on the right of Fig. 4, show that now both the longitudinal and lateral displacements are in very good agreement with the full simulation.

Truck model

The truck model considered here represents an extension of a benchmark problem proposed in [17]. More specifically, we replaced in the original model the rigid load area by an elastic structure and added another tire and a load. Thus, as shown in Fig. 5, the resulting model consists of 8 rigid and one elastic body. For the 2D-finite element discretization of the PDE describing the displacements of the load area the Matlab PDE Toolbox [11] was applied under the assumption of plane stresses. As a result the gross motion is characterized by $n_p = 16$ coordinates, and there are $n_q = 198$ elastic variables. The load and the rotational

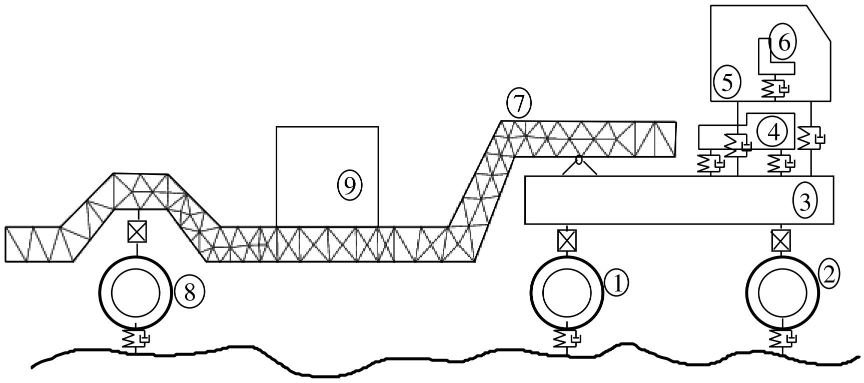

Figure 5: Truck model with eight rigid bodies and one elastic body (load area 7).

joint between bodies 3 and 7 require $n_\lambda = 5$ constraint equations. In contrast to the slider crank example, the truck model has dampers as interconnection elements between the bodies, and, hence, does involve dissipation.

An eigenvalue analysis shows that the first eigenfrequency of the elastic body is about $100.43[rad/s]$ or 16 Hz. It would be feasible to perform here a reduction to eigenmodes. Instead we employ this model to show that the algorithm of Section 4 works well also for large systems. At the same time, we note that a space discretization, different than that produced by the 3 node triangular elements of the PDE Toolbox, may well be desirable for a slim body of the form of the load area. This is a topic of finite element analysis and will not be considered here.

After exporting the necessary finite element data, as the mass and stiffness matrices from Matlab to Fortran, we ran several simulations to test the algorithm of Section 4. For this one starts on a smooth road segment which then turns into a rough segment expressed by a Fourier approximation as given in [17]. Due to the 2D space discretization, the overall system is very stiff and explicit time discretization schemes do not work any longer. Even implicit solvers, such as RADAU5, [4], face severe problems since the iteration matrix is badly scaled and order reductions may occur (see, e.g., [10] for a discussion of Runge-Kutta methods for stiff mechanical systems). By careful adjustment of the tolerances and other parameters, RADAU5 succeeded in computing a full solution of the index 2 formulation of (1). Fig. 6 shows a comparison of this full solution q and the asymptotic approximation q^a computed by the algorithm of Section 4. It may be noted that the computing time for the latter algorithm was only about 8% of that of the RADAU5 run. Both solutions differ only in the third digit, as indicated on the right of Fig. 6 for the displacements of a particular node chosen near the joint between bodies 3 and 7.

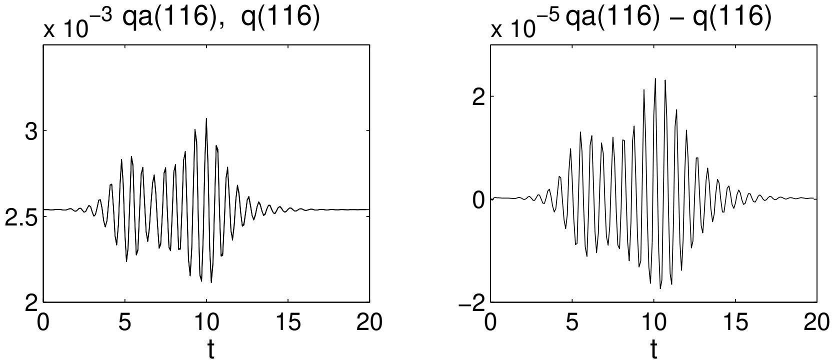

Figure 6: Comparison of vertical displacements at node 17 in $[m]$.

References

[1] Bornemann, F.A.: *Homogenization in Time of Singularly Perturbed Conservative Mechanical Systems* . Habilitationsschrift, ZIB Berlin, 1997

[2] Cartmell, M.: *Introduction to linear, parametric, and nonlinear vibrations.* Chapman and Hall 1990

[3] Géradin, M.: *Computational aspects of the finite element approach to flexible multibody systems.* In Schiehlen W. (Ed.): Advanced Multibody System Dynamics, 337-354, Kluwer Academic Publishers: Stuttgart 1993

[4] Hairer, E., Wanner, G.: *Solving Ordinary Differential Equations II.* 2nd ed., Berlin, Heidelberg: Springer 1996

[5] Hughes, T.J.: The Finite Element Method. Prentice Hall, Englewood Cliffs 1987

[6] Lion W., de Swart J., van der Ween, W.: Test Set for IVP Solvers, Report NM-R9615, CWI Amsterdam, 1996, `http://www.cwi.nl/cwi/projects/IVPtestset.shtml`

[7] Jahnke, M., Popp, K., Dirr, B.: *Approximate analysis of flexible parts in multibody systems using the finite element method.* In Schiehlen W. (Ed.): Advanced Multibody System Dynamics, 237-256, Kluwer Academic Publishers: Stuttgart 1993

[8] Kim, S., Haug, E.: *Selection of deformation modes for flexible multibody dynamics.* Mech. Struct. Mach. 18, 565-586 (1990)

[9] Lubich, C.: *Extrapolation integrators for constrained multibody systems.* Impact Comp. Sci. Eng. **3**, 213-234 (1991)

[10] Lubich, C.: *Integration of stiff mechanical systems by Runge-Kutta methods.* ZAMP **44**, 1022-1053 (1993)

[11] Nordmark, A.: The Matlab PDE Toolbox. The Mathworks Inc., 1995

[12] Rheinboldt, W.C.: *MANPAK: A set of algorithms for computations on implicitly defined manifolds.* Computers and Math. Appl. 32, 15-28, 1996

[13] Rheinboldt, W.C.: *Solving algebraically explicit DAEs with the MANPAK manifold algorithms.* Computers and Math. Appl. 33, 31-43, 1996

[14] Sachau, D.: *Berücksichtigung von flexiblen Körpern und Fügestellen in Mehrkörpersystemen zur Simulation aktiver Raumfahrtstrukturen.* Diss., Universität Stuttgart, Institut A für Mechanik, 1996

[15] Schiehlen, W.O. (Ed.): *Multibody System Handbook.* Springer: Berlin 1990.

[16] Shabana, A.: *Computer implementation of flexible multibody equations.* In Pereia, M., Ambrosio, J.: Computer Aided Analysis of Rigid and and Flexible Mechanical Systems, 325-349, Kluwer Academic Publishers: Dordrecht 1994

[17] Simeon, B., Grupp, F., Führer, C., Rentrop, P.: *A nonlinear truck model and its treatment as a multibody system.* J. Comp. Appl. Math. 50, 523-532 (1994)

[18] Simeon, B.: *DAE's and PDE's in elastic multibody systems.* submitted to Annals of Numer. Math.

[19] Simeon, B.: *Modelling a flexible slider crank mechanism by a mixed system of DAEs and PDEs.* Math. Modelling of Systems **2**, 1-18 (1996)

[20] Wallrapp, O.: *Standardization of flexible body modelling in MBS codes.* Mech. Struct. Mach. 22, 283-304 (1994)

[21] Walter, W.: *Differential and Integral Inequalities.* Springer 1970

[22] Yan, X.: *Singularly perturbed differential-algebraic equations.* Techn. Report ICMA 94-192, Univ. of Pittsburgh 1994